arXiv:astro-ph/9810156v3 5 May 1999

X-ray outburst of CI Cam/XTE J0421+560: RXTE observations

Revnivtsev M.[1], Emelyanov A.[1], Borozdin K.[1,2]
[1] – Space Research Institute, Moscow, Russia
[2] – Los Alamos National Laboratory, Los Alamos, NM 87545, USA

ABSTRACT

We present the results of observations of XTE J0421+560 X-ray transient with Rossi X-ray Timing Explorer in the beginning of April 1998. Lightcurve, obtained by ASM all-sky monitor, shows unusually fast decrease in the object's luminosity. Spectra from series of observations by PCA and HEXTE experiments were studied in detail. Two emission line regions with energies around 6.5 keV and around 8 keV have been mentioned in the spectra. The possibility of generation of the observed emission in relativistic plasma jet has been discussed. Some analogy is found with known Galactic jet source SS433.

1. Introduction

The X-ray transient XTE J0421+560 was discovered on Mar. 31, 1998 with All Sky Monitor aboard RXTE. According to ASM data the flux from the source in 1-12 keV energy range was rising quickly from 40 mCrab Mar. 31.36 to 1880 mCrab Apr. 1.04(Smith&Remillard 1998). PCA and HEXTE observations started Apr. 1.08, 1998 and confirmed the ASM results (Marshall&Strohmayer, 1998). The new X-ray source was localized by PCA with coordinates: Ra=$4^h19.6^m$, Dec=$+56^o00^{'}$ (Marshall&Strohmayer,1998b). The lightcurve of the source was characterized by extremely fast rise up to the maximum with subsequent, also unusually fast decay of the flux. The observations by ASCA and BeppoSAX satellites showed the presence of the strong emission line around 6.7 keV.

The radio observations of Apr. 1, 1998 revealed the bright radio source at the location R.A.= $4^h19^m42^s.05$ +/- $0^s.03$, Dec. = $+55^o59^{'}58^{"}.6$ +/- $0^{"}.5$, 2000 equinox (Hjellming&Mioduszewski, 1998a). The radio source, which position is coincident with that of symbiotic star CI Cam (Wagner&Starrfield, 1998) was proposed to be the radio counterpart of X-ray transient XTE J0421+560. The radio images obtained on Apr 5 and 6, 1998 revealed that the CI Cam radio source had become resolved. The VLA images showed the extended radio emission that had the appearance of a roughly symmetrical S-shaped

twin-jet, strikingly similar to the radio jets of SS 433 (Hjellming&Mioduszewski, 1998c). The outermost pair of emission components was separated by ~ 0.33". Assuming the expansion started on Mar. 31.6, 1998 the proper motion of the components is 26 mas/day. Assuming a distance of 1 kpc (Chhikvadze 1970), this corresponds to apparent tangential velocity $v \sim 0.15c$.

Optical spectroscopy of CI Cam showed the strong emission lines of H, He I, Fe II. However, none of the lines showed double peak profile, which is typical for the accretion disk emission in X-ray binaries and cataclysmic variables. These results are consistent with CI Cam/XTE J0421+560, but suggest that it might be unusual X-ray symbiotic star(Garsia et al., 1998).

2. Observations and analysis

In the present work we used the data obtained by Rossi X-ray Timing Explorer (Bradt, Swank&Rothschild, 1993). The data was retrieved from the XTE GOF at GSFC. The ASM light curves were used as provided by the XTE GOF. The RXTE has a payload of two coaligned spectrometers – PCA and HEXTE – that provides the broad band spectral coverage for energy range from 3 to ~ 200 keV and All Sky Monitor, that give a possibility to follow the long term behavior of the source with nearly complete time coverage within 1-12 keV energy band.

The PCA and HEXTE data was treated with standard FTOOLS v.4.1.1 package tasks. To estimate the PCA background we run the latest version of task *pcabackest* v.2.0 (Stark 1998). We applied new $L7/240$ model to the observations, when the source was extremely weak (Apr. 8–9, 1998), and VLE based background model – for others. In our spectral analysis we used PCA rmf matrix v.3.3 (Jahoda 1998, see also the *erratum* Jahoda 1998a). The analysis of the Crab nebula spectra had confirmed, that the systematic uncertainties of the matrix are less than 1%. We would like to note, that PCA effective area is substantially decreased after ∼3–4 keV to the lower energies, so the estimation of N_H value with PCA should be treated with care. To account roughly for the uncertainty in the knowledge of the spectral response, 1% of systematic error had been added to the statistical errors for each PCA channel. All spectra had been corrected for deadtime according to Zhang&Jahoda, 1996.

For the spectral analysis of the HEXTE data the version 2.6 (released Mar. 20, 1997) of the response matrix had been taken. The background for each cluster of HEXTE detectors was estimated using the off-source observations. Only the data above 15 keV were taken

into account because of the uncertainties of the response matrix below this energy. At the high energy end the spectrum was cut at $\sim 80 - 150$ keV depending on the brightness of the source in order to avoid significant influence from the background subtraction uncertainty. The deadtime correction had been performed using hxtdead FTOOLS task for all observations.

The brief information about the RXTE observations of the source are presented in Table 1.

3. Lightcurve

The lightcurve of the source in various energy bands is shown in Fig. 1. The peculiar point in this figure is that the ASM data in the lowest energy band 1.3-3.0 keV show the feature that looks like secondary peak around the 5th day after the beginning of the outburst (Fig.1a). Similar "kick" feature is frequent for the lightcurves of the X-ray novae in standard X-ray band, but in our case the feature is seen only in the soft X-ray band ($<$ 3 keV) while the flux at higher energies is decreasing monotonically . Note, that flaring in softer energy band was observed also by ASCA observatory around the same date (Ueda et al., 1998b)

In the lower panels the hardness ratios of the source are presented. The flux decay during the period Apr.1-3 in the total ASM energy band can be approximated with the exponential law with e-fold time $\sim$0.6 day, later on the e-fold time increases to $\sim$1.1 day. The example of the source flux decay during the first session of observation by the PCA and HEXTE is shown in the Fig.2. During this observation e-fold times were $\sim$0.57 day for the PCA energy band and $\sim$0.28 day for the HEXTE energy band.

4. Energy spectrum

The source spectrum in the 3–100 keV energy band can by approximated by a power law with the exponential cutoff at higher energies: $dN \sim E^{-\alpha} e^{-\frac{E}{E_{cut}}} dE$. Extremely strong emission line is present in the spectrum at energies around 6.4–6.7 keV. Similar spectral shape was found by ASCA and BeppoSAX observatories for their observations (Ueda et al., 1998, Orlandini et al., 1998). However, for the PCA spectra this model leaves the significant residual at the energies around 8 keV with the amplitude ($\sim$4–6%, see Fig.3), which is sufficiently higher than the response matrix uncertainty. Because of the presence of very bright emission line at the energies 6.4–6.7 keV and low energy resolution of PCA

in this energy band (∼1 keV), the quality of the data approximation at the energies ∼8 keV will strongly depend on the accuracy of used photon redistribution matrix (definite part of the response matrix). The analysis, carried out with collaboration of Keith Jahoda (RXTE/PCA team) have showed, that the unaccuracy of the matrix is not worse than ∼1% and the observed excess around 8 keV should be considered as real intrinsic spectral feature of the source. An addition of the emission line at energy ∼8.1 keV significantly improves the quality of the data approximation in terms of χ^2 statistics – χ^2 value reduces by ∼40 with the systematic uncertainties included and by ∼9000 with statistical errors only. As a result, the best fit analytical model consists of a power law with high energy exponential cutoff, low energy absorption, and two emission lines. The parameters of this model for different sessions are given in Tables 2 and 3. We would like to note, that the spectral results of PCA with response matrix 3.3 have relative uncertainties in energy around 0.02 keV at the energies 6–8 keV, but the uncertainties in absolute values is slightly higher, it can be estimated to be $\sim 1\% \sim 0.07$ keV (Jahoda 1998, private communication). One should bear this in mind, while tring to localize the lines in the spectrum.

Combined spectra of PCA and HEXTE experiments for three different observations are presented in Fig.4 (in the Fig.4 *meka* model was used to approximate the line emission, see below). The spectra can be approximated satisfactorily by the aforementioned model. Note, hovewer, that because of calibration uncertainties the photon indexes of the Crab spectra of PCA and HEXTE have slightly different values (on ~ 0.05–0.1), therefore some deviations in spectral shapes between two experiments can be expected.

Due to the decrease of the flux and the softening of the spectrum from XTE J0421+560 the source had not been detectable by HEXTE after Apr.4, 1998.

The shape of the spectra is close to the spectrum of the emission of optically thin plasma (*bremsstrahlung*), but cannot be satisfactorily fitted by this model with single temperature. Possible interpretations of this fact could be fast change of the temperature affecting the intergral spectrum or non-equilibrium state of the emitting plasma.

It is worth to note several features of the obtained spectra: 1) the absorbtion value N_H, that characterizes the low energy cutoff in the spectra is changing from $\sim 4.8 \times 10^{22}$ on Apr.1.04, $\sim 6.5 \times 10^{22}$ Apr.1.35, to $\sim 1.5 \times 10^{22}$ the day after and then became insignificant; 2) the slope of the power law fit increases and the cutoff energy decreases with time, which shows the cooling of the emission medium; 3) the center of the broad emission line 6.5–6.7 keV fluctuates to the higher energies. (see Fig. 5 and 3).

Below we discuss the possible interpretation of these and other observational results.

5. Discussion

The X-ray transient source XTE J0421+560/CI Cam has several featues that make it different from the other known X-ray transients. The most striking difference, which has been repeatedly mentioned in the related publications, is an extremely fast evolution. Mean value of e-folding decay time for know X-ray transient is $\sim$ 30 days (see Wan Chen et al. 1997), whereas for XTE J0421+560 it is $\sim$ 0.5–1 day. Possibly, the main difference is the nature of the compact object in these systems. CI Cam is known to be symbiotic binary, i.e. the binary which composed by red giant and an accreting white dwarf. The most probable cause of the flares in these systems is considered to be the thermonuclear outburst on the surface of the white dwarf. Unstationary accretion in the system is proposed as an alternative mehanism for the flares generation (see e.g, review of the models by Mikolajewska&Kenyon 1992).

It should be noted that the X-ray observations of XTE J0421+560 do not demonstrate the features, which is usually attributed to the presence of the accretion disk in the system, – QPO, or characteristic Very Low Frequency Noise in the power spectrum, or typical soft component in the energy spectrum. Moreover, the analysis of the light curve of the source on the various time scales (from hundreds of microseconds up to hundreds and thousands of seconds) do not reveal the significant variability of the source flux different from the main trend of the flux decay. This result is consistent with observations of ASCA and SAX (Ueda et al., 1998b, Frontera et al.,1998). Hovewer, according to SAX and ASCA data X-ray flux in the 0.5-1 keV energy band do has variability on the scales of hundreds of seconds and hours.

The character of the source flux variability could be an evidence that the soft and hard X-ray components are forming in the geometrically different parts of the system. The dimension of the region, where the hard component is formed, should be larger than $R \sim c_s\tau \sim 10^8 \times 100 = 10^{10}$ cm, here c_s – the sound velocity in the medium with $T \sim 10$ keV, while the region, where the soft component is formed, must be less than $\sim 10^{10}$ cm in size.

5.1. Continuum spectrum

As it has been mentioned above, the best fit model for continuum spectrum is the power law with high energy cutoff at the energies $\sim$5–13 keV. The spectrum of this type can be formed in the cloud of optically thin hot plasma, that has non-uniform temperature distribution. It should be noted that this form of the spectra is completely different from

that of the many other X-ray Novae - black hole candidates, where X-ray emission was detected up to hundreds keV (see e.g., Sunyaev et al., 1994; Tanaka&Shibazaki, 1997).

5.2. Low energy absorption

The spectra, obtained during the first two days after the beginning of the outburst demonstrate the presense of significant low energy absorption. The N_H value was increased from $N_{HL} \sim 4 - 5 \times 10^{22}$ on Apr.1.04, 1998 (model dependent value) to $N_{HL} \sim 6 - 7 \times 10^{22}$ on Apr. 1.35, 1998 and then decreased to $N_{HL} \sim 1 - 2 \times 10^{22}$ one day later and had become insignificant during later observations. It is quite natural to interpret that at the beginning of the outburst the X-ray source had been embedded within dense and cold cloud, which later on became less dense and, consequently, more transparent as a result of mass loss and/or temperature heating. Lightcirves of the object, obtained in X-ray, optical and radio bands may also be considered as an evidence of the cloud density decrease with time(Frontera et al.,1998).

The radio observations of the relativistic jet structures (Hjellming&Mioduszewski, 1998c) supports an idea of significant outflow of the matter from the central object of the system XTE J0421+560 during the outburst. It is interesting to estimate the dimensions and the density of the cloud assuming its cylindrical shape.

Let us assume, that the cloud forms a cylinder with radius R, length L expanding along the cylinder axis, perpendicular to the line of sight (see below the discussion of orientation of the jets). We accept for simplicity that the cloud has the uniform distribution of the density. The low energy absorption observed can be caused either by bremsstrahlung self absorption or by photoabsorption in the cool outer region of the cloud. With soft X-ray instrument in hand it would be possible to distinguish between these two possibilities because of its different influence on the source spectrum. Unfortunately, PCA do not allows to do it.

If the low energy cutoff in the spetra of XTE J0421+560 is due to photoabsorption, then we can make some simple estimations on the cloud dimensions. The value of photoabsorption can be approximated as $N_H \sim CNR$, where $C < 1$– part of the cloud which contribute to the N_H value, N– density of the cloud. Emission measure in the cloud EM is given by:

$$EM = \int N^2 dV = N^2 V \sim N^2 \pi R^2 L. \quad (1)$$

Then we obtain:

$$L \sim \frac{C^2 EM}{N_H^2} \sim \frac{C^2 6 \times 10^{59}}{(5 \times 10^{22})^2} \sim 2.4 C^2 \times 10^{14} cm. \quad (2)$$

Taking into account that this value is just order-of-magnitude evaluation of cloud length we can say, that our estimation is consistent with the observed expansion rate of the cloud in this direction $\sim 1 \times 10^{13}$ cm/hour if $C \sim 0.1 - 0.2$. It should be noted, that if the radiation goes through the cold surrounding medium, the weak fluorescent line of Fe at the energy ~ 6.4 keV should be formed (see the discussion of this item below and also in Ueda et al., 1998b). We emphasize that the discussed model should not be considered as ultimate, but as one of the possible ones.

Under assumptions that there is no energy supply to the cloud after the maximum of the lightcurve is reached, and that to the moment of sufficient flux decrease (after ∼3–4 days after the peak) the cloud have lost a significant part of its energy, we can estimate the density of the cloud. Let us take the characteristic time of the flare to be τ ∼1–2 days ($\sim 10^5$ s). From the energy balance of the cloud (see also Ueda et al., 1998b):

$$\frac{NkT}{\tau} \gtrsim AN^2\sqrt{T}, A \sim 1.7 \times 10^{-27} erg/s \quad (3)$$

and

$$N \lesssim \frac{k\sqrt{T}}{\tau A} \sim 10^{10} cm^{-3} \quad (4)$$

Accepting this value of the density, we can evaluate the transverse size of the cloud $R \sim N_H/NC \sim 0.5 - 1.0 \times 10^{13}$ cm and total mass of the erupted matter $M \sim m_p NV \sim m_p EM/N \sim 8 \times 10^{25}g\sim 4 \times 10^{-8} M_\odot$. The obtained estimated value of R is consistent with the free expansion of the cloud in this direction $R \sim c_s \tau \sim 10^{13}$ (c_s – the sound velocity of the gas with the temperature $kT \sim 10$ keV).

5.3. Emission lines origin

The most likely, that the observed lines in the spectrum of XTE J0421+560 has been generated in the optically thin emission of the hot plasma cloud. Alternative mechanisms of line formation – the propagation though the medium or the reflection – is less probable, because of huge equivalent width of the observed line. Besides, if the propagation or the reflection would be responsible for the line formation then the strong absorption edge (EW> 700 eV) would be formed at energies above the line. The lack of such a feature

moves us to believe that both the continuum spectrum, that extends up to the 100 keV and the observed emission features are formed in the hot optically thin plasma cloud. However, the PCA data show that the model of emission of optically thin plasma with lines with kT ∼10–15 keV doesn't give a good approximation of the spectra ($\chi^2 = 187.8$ for 41 d.o.f for the first observation). High χ^2 value is mainly driven by the fact that the model fails to predict the right ratio between the fluxes detected from different lines. If we take two-component model that consists of the emission of optically thin plasma cloud without emission lines (*bremsstrahlung*) with kT ∼14 keV and the emission of the plasma cloud with emission lines (*meka*) with kT ∼5 keV, then we will get much better fit in terms of χ^2 (∼ 16 for 38 d.o.f.). It should be noted that in order to get the good approximation one should take into account the Doppler shift $z \sim 0.03$ (see. Table 4 and the discussion below). So, we believe that the spectrum of XTE J0421+560 consists of (at least) two components, one of which describes the continuum spectrum extended up to ∼100 keV and the second one represents the region, where emission lines are formed. The difference between the characteristic temperatures of these two components during whole outburst may hint on the fact that they are emitted by the geometrically different regions of the system (see also analysis of the flux variability above). The best fit parameters for the discussed model are presented in Table 4. The combined PCA and HEXTE spectra shown in Fig.4.

5.4. The emission line positions in the spectra

The PCA data demonstrate that the spectrum of the source has strong emission line features at the energies around 6.5–6.7 keV and around 8 keV. The existence of the strong line at the energy ∼6.7 keV has been reported by all instruments which observed XTE J0421+560 and had needed capabilities in this energy range. New and interesting results of the present work is the shift of the central energy for Fe-line complex and the detection of additional significant line-shaped emission around 8 keV [1]. In the light of recent radio observations of relativistic jets it looks attractive to interpret the observed drift of Fe-line in terms of the change of Doppler effect value for relativistically moving plasma. This interpretation is in agreement with results obtained by ASCA. Estimated velocity of the expansion is equal to $\sim 0.03c$ for the observation on April 1, with following decrease of this value leading to observed shift of line centrum to higher energies. If an initial shift is really caused by Doppler effect, then an orientation of the cloud must be equal to $\sim arctg(0.15/0.03) \sim 80^o$ relative to the line of sight. Thus the expected shape of the jets should be close to symmetrical as it was really observed in radio band. Our expansion

[1] As it was mentioned above, 8 keV line emission can be well approximated by *meka* model

velocity estimation is in principal agreement with ASCA results (Ueda et al., 1998b).

One serious argument against this interpretation is the lack of blue-shifted line component in the spectra. Emission line ~ 8 keV is hardly can be interpreted as such a component, because, even taking into account an uncertainty in its position, its intensity is still much weaker than for 6.5-6.7 keV line. Hovewer, one should take into account that PCA energy resolution ($\sim 18\%$) does not allow to distinguish between multiple lines which might present in this energy band.

It is remarkable, that similar shift in emission line energy up to $\gtrsim 7$ keV had been observed for SS433 source during its observation by EXOSAT and had been interpreted in terms of Doppler effect (Watson et al., 1986). But in that case only blue-shifted component had been detected, and the absense of red-shifted line was explained for the screening of the emitting region by the accretion disk.

If the change in the energy observed for 6.7 keV emission line is due to the relativistic motion of an emitting cloud of optically thin plasma, then the decrease in ΔE with time can be attributed to the decrease of the velosity of the cloud or to the precession of the jet axis, in the analogy with SS433 system. Hovewer, the time dependence of the emission measure (see below) does not show any significant decrease in the expansion velosity, which is an argument in favor of the precession. In this case a period of the precession is > 10 days (in comparison with ~ 164 days for SS433). S-shaped structure observed in radio band is another argument, which suggest that the change in observed expansion velosity is due to the change of the projection of the expansion vector to the line of sight.

As an alternative explanation of the observed shift of the line to lower energies one can consider a presence in the spectrum of fluorescent Fe-line at 6.4 keV, which is generated during the passage of X-rays through cold dense cloud surrounding the X-ray source. It is possible that an equivalent width of this line has decreased significantly during later observations, which resulted to the shift of the centrum of broad emission feature detected by PCA. The trend of low-frequency absorption discussed above is in favor of this interpretation. Hovewer, it looks like higher optical depth of cold cloud is needed to form 6.4 keV line with sufficient width. This model is also discussed by Ueda et al.(1998) as a possible interpretation of ASCA results.

The spectral feature observed around 8 keV could be attributed to the emission line of highly ionized Ni or to Fe K_β line complex. While an emission in Fe line with energies ~ 6.7 keV has been widely observed from many X-ray sources, the detection of Ni-line is quite unusual result. We believe, that this detection became possible in this case only because of extreme brightness of the source and unusually high significance of line emission component

in its spectrum combined with high sensitivity of PCA experiment.

5.5. Evolution of X-ray spectra

To trace the changes of physical parameters for an emitting system we have applied two-component model compoused of the component of optically thin plasma emission without lines and another component of optically thin plasma with line emission (as has been discussed above). We have used PCA data only, because its sensitivity is high enough to trace spectral parameters change for small exposure times. We find best fit parameters for spectra integrated over 400-sec time intervals for the first three observational sessions, when the brightness of the source have been at maximum, and one integrated spectrum for the rest of the sessions. The dependencies obtained for emission measure and temperature parameters are shown in Figures 7 and 8. It is evident from Fig.7 that after $\sim$ 30 hours after the beginning of the outburst emission measure for both components is decreasing as $EM \sim t^{-2}$, while overall behaviour of this parameter can be described as $EM \sim (1 + (t/t_0)^{\alpha})^{-1}$, where $\alpha \sim 2.17$ for the first component (bremsstrahlung without lines) and $\alpha \sim 2.25$ for the second component with lines (meka). There is no evidence in Fig.7 that expansion velosity is decreasing with time.

If we assume that cloud mass $M \sim m_p NV$ is constant, then its internal thermal energy will depend of the temperature T only, and emission measure - of density N only. In this case the volume of the cloud is proportional to the emission measure: $V \sim EM^{-1}$. From the observations the time dependence of the emission measure parameter is given by $EM \sim (1 + (\frac{t}{t_0})^{\sim 2})^{-1}$. Then the cloud volume will increase with time as $V \sim (1 + (\frac{t}{t_0})^2)$. We note, that index value $\alpha \sim 2 < 3$ is an indication of non-isotrop or collimated expansion of the cloud.

The temperature vs time dependence is quite complicated (Fig.8), but one can mention two main features to describe it. During the first 20-30 hours after March 31.6 the temperature of the components remain relatively constant in comparison with significant change of the emission measure. After $\sim$ 30 hours, the temperature is decreasing as $\sim t^{-0.6}$.

5.6. The comparison with other X-ray sources

While XTE J0421+560 have a set of prominent differencies from other X-ray transients, radio observations have shown an evident similarity between this source and SS433, well-known Galactic object emitting relativistic plasma jets. An analogy between two

sources is revealed itself in X-ray band also, because both of them have similar continuum spectra and strong emission lines aroun 6.7 keV. Furthermore, the shift of line centra with time is detected for both sources which might be explained in terms of Doppler shift in line energy. The important difference between two sources is a fact that XTE J0421+560, contrary to SS433, is a transient object, which had been active in X-ray and radio bands for few days only.

We would like to note, that rapid decrease of X-ray flux with simultaneous softening of the spectrum, as well as shift of the maximum of energy emission with time for different bands of electromagnetic spectrum is typical also for gamma-burst afterglows.

6. Conclusion

The observations of X-ray transient XTE J0421+560, which is an X-ray counterpart of symbiotic binary CI Cam, by RXTE experiments give a set of important and unexpected results. First of all, the source attracted the attention because of unusually fast rise of its X-ray flux, which was followed by also too fast decline after the maximum passage. During 10 days of observations by PCA and HEXTE experiments the flux from the source had been decreased by more than two orders of magnitude.

One interesting result is the detection of soft X-ray flare, which was not correlated with the flux change in harder energy range.

The source spectrum in 3-150 keV band can be approximated by power-law with an exponential cut-off at higher energies. The spectrum of this shape can be generated in the cloud of non-thermalized optically thin plasma. The softening of the spectrum (or decrease of the effective temperature) with the decrease of flux has been mentioned.

The changes in low-energy absorption in the spectrum is probably due to the decrease in density of the cold cloud, which surrounds X-ray source. Initial mass of the cloud can be estimated as $\sim 4 \times 10^{-8} M_{\odot}$.

The emission lines have been detected at energies 6.5-6.7 keV and around 8 keV. Discovered shift of the 6.7-keV line to lower energies can be explained either as Doppler-effect for moving media, or as generation of another, 6.4-keV emission line in cold cloud, density of which evolved with time. If the reason is Doppler-effect, then this is the second time, after SS433, when an X-ray emission generated by relativistic jet plasma is observed in our Galaxy. In this case the cloud is expanded under angle $\sim 80^{o}$ to the line of sight. The appearance of the line near 8 keV is probably due to the emission of highly ionized Ni

or Fe K_β line, and, as far as we know, is detected for the first time for Galactic sources.

Authors thank E.Churazov for helpfull advises and comments, S. Sazonov, S. Trudolyubov and A. Finoguenov for extensive discussions of the presented results. Authors especially thank Keith Jahoda for the help in the analysis of spectral capabilities of PCA. Also we thank Y.Ueda and H.Inoue for the possibility to get to know ASCA results before its publication. The research has made use of data obtained through the High Energy Astrophysics Science Archive Research Center Online Service, provided by the NASA/Goddard Space Flight Center. This work was partly supported be RBRF grant 96-15-96343.

7. References

Bradt H., Rotshild R., Swank J. Astron. Astrophys. Suppl. Ser., 1993, vol. 97, no. 1, p. 355-360.

Chen Wan, Shrader C., Livio Mario Astrophys. J., 1997, v.491, p.312.

Chkhikvadze Ja. Astrofisika 6, 65, 1970.

Frontera F., Orlandini M., Amati L., Dal Fiume D., Masetti N., Orr A., Parmar A., Brocato E., Raimondo G., Piersimoni A., Tavani M., Remillard R. Astron. Astrophys. 1998, see also astro-ph/9809287

Hjellming R., Mioduszewski a. IAU Circ. No. 6857, 1998a

Hjellming R., Mioduszewski b. IAU Circ. No. 6862, 1998b

Hjellming R., Mioduszewski c. IAU Circ. No. 6872, 1998c.

Jahoda K. 1998a, http://lheawww.gsfc.nasa.gov/ users/ keith/ pcarmf.html

Jahoda K. 1998b, http://lheawww.gsfc.nasa.gov/users /keith/pcarmf_ft41.erratum

Marshall F., Strohmayer T. IAU Circ. No. 6857, 1998

Mikolajewska Joanna, Kenyon S. MNRAS 1992, vol. 256, no. 2, p. 177-185.

Orlandini M., Dal Fiume D., Frontera F., Antonelli L., Piro L., Parmar A. IAU Circ. No. 6868, 1998

Smith D., Remillard R. IAU Circ. No. 6855, 1998

Stark 1998, http://lheawww.gsfc.nasa.gov/ ∼stark/ pca/ pcabackest.html

Sunyaev R., Borozdin K.,Aleksandrovich N., Arefev V., Kaniovskii A., Efremov V., Maisack M., Reppin C., Skinner J. Astr. Lett. vol.20, no.6, p. 777, 1994

Ueda Y., Ishida M., Inoue H., Dotani T., Lewin W.H.G., Greiner J. IAU Circ. No. 6872, 1998a.

Ueda Y., Ishida M., Inoue H., Dotani T., Greiner J., Lewin W.H.G. Astrophys. J. 1998b, see also astro-ph/9810100.

Wagner R., Starrfield S. IAU Circ. No. 6857, 1998

Watson M., Stewart G.,Brinkmann W., King A. MNRAS 1986, 222, 261-271.

Zhang W., Jahoda K. 1996, http://lheawww.gsfc.nasa.gov/ users/ keith/ deadtime/deadtime.html

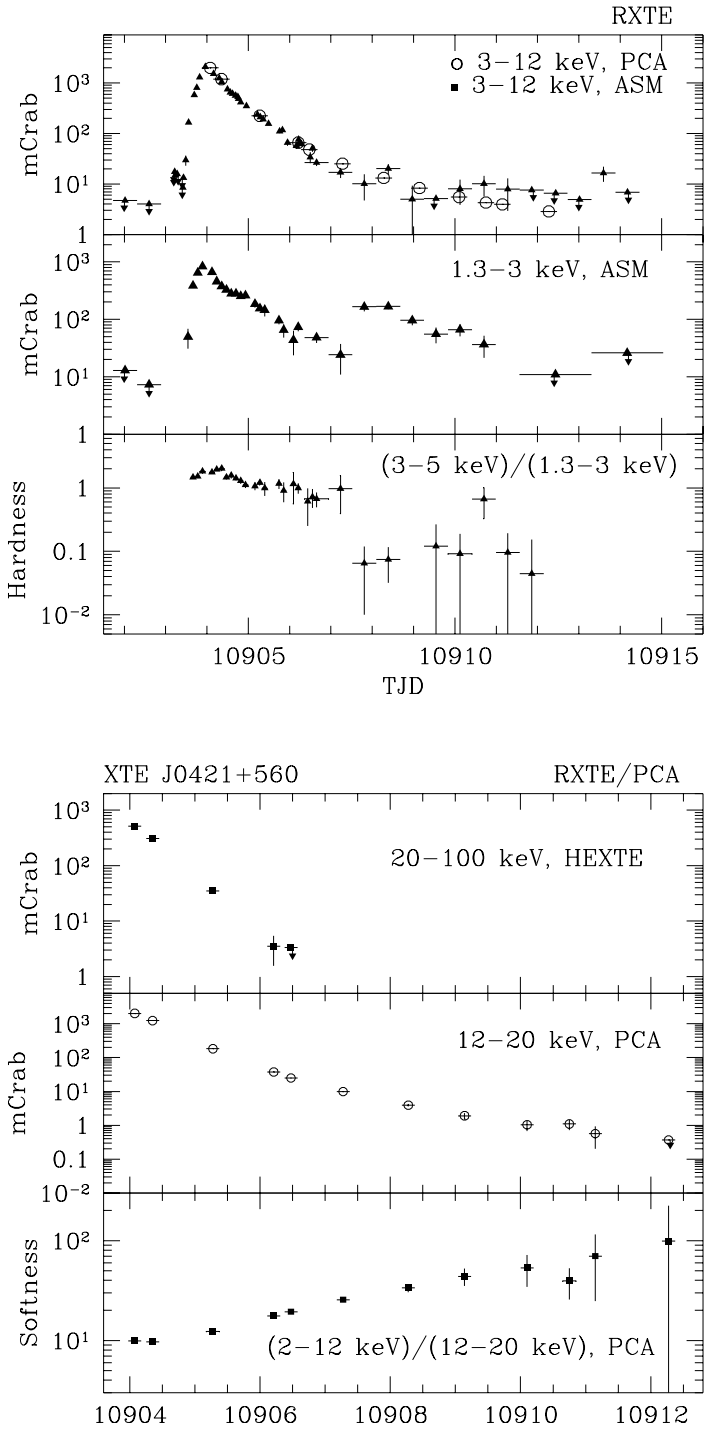

Fig. 1.— The lightcurve of XTE J0421+560 according to RXTE data

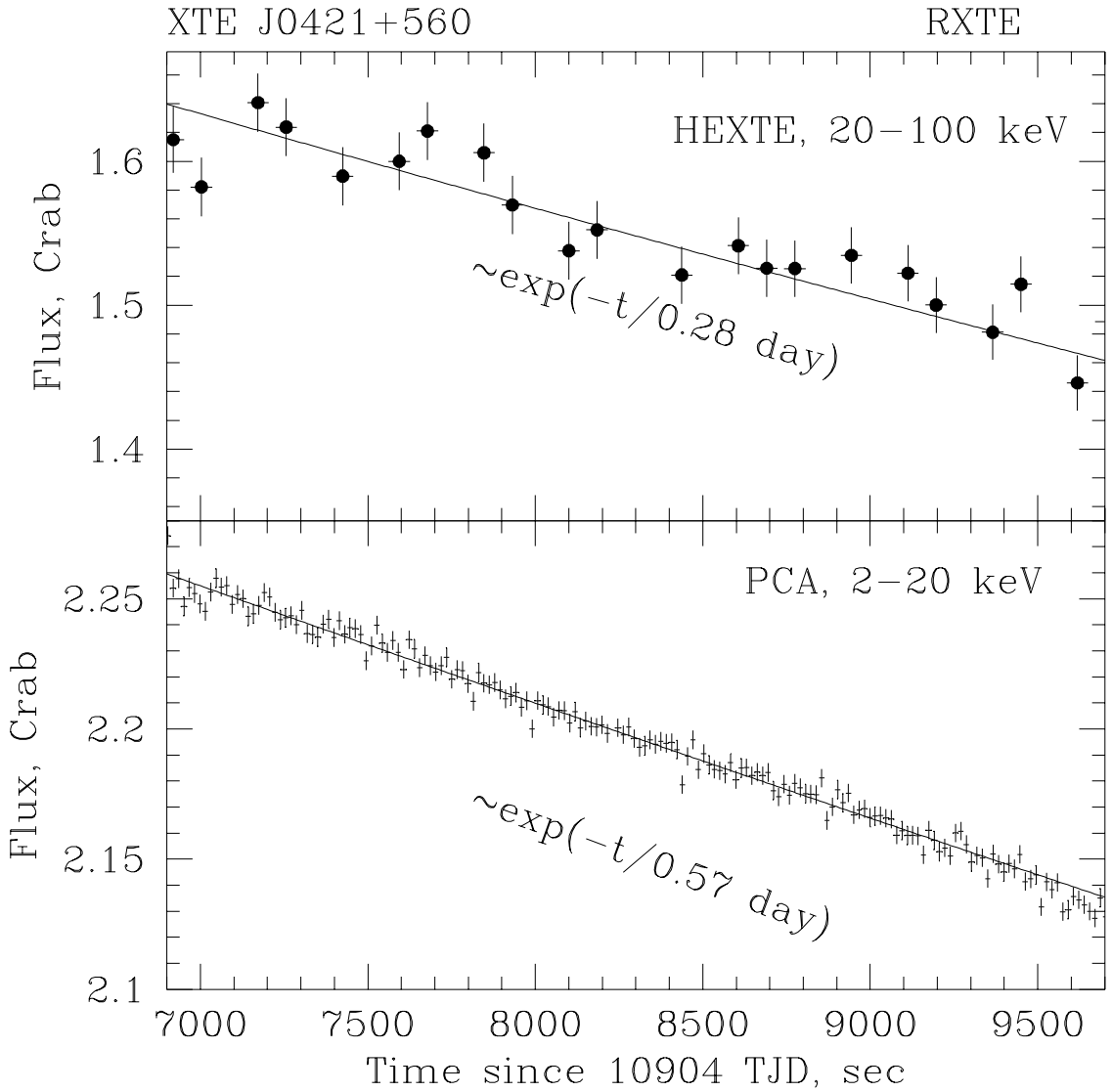

Fig. 2.— The lightcurve of XTE J0421+560 during the part of the first observation (PCA and HEXTE data). The solid lines show approximation $e^{-\frac{t-t_o}{\tau}}$, where τ ∼0.56 day for PCA points (lower panel) and τ ∼0.28 day for HEXTE points (upper panel), t_o was taken to be Mar. 31.6, 1998. One can see that the flux from the source do not demostrate significant variability on the time scales 20–1000 s. The χ^2 value for the PCA points – 182 for 162 points.

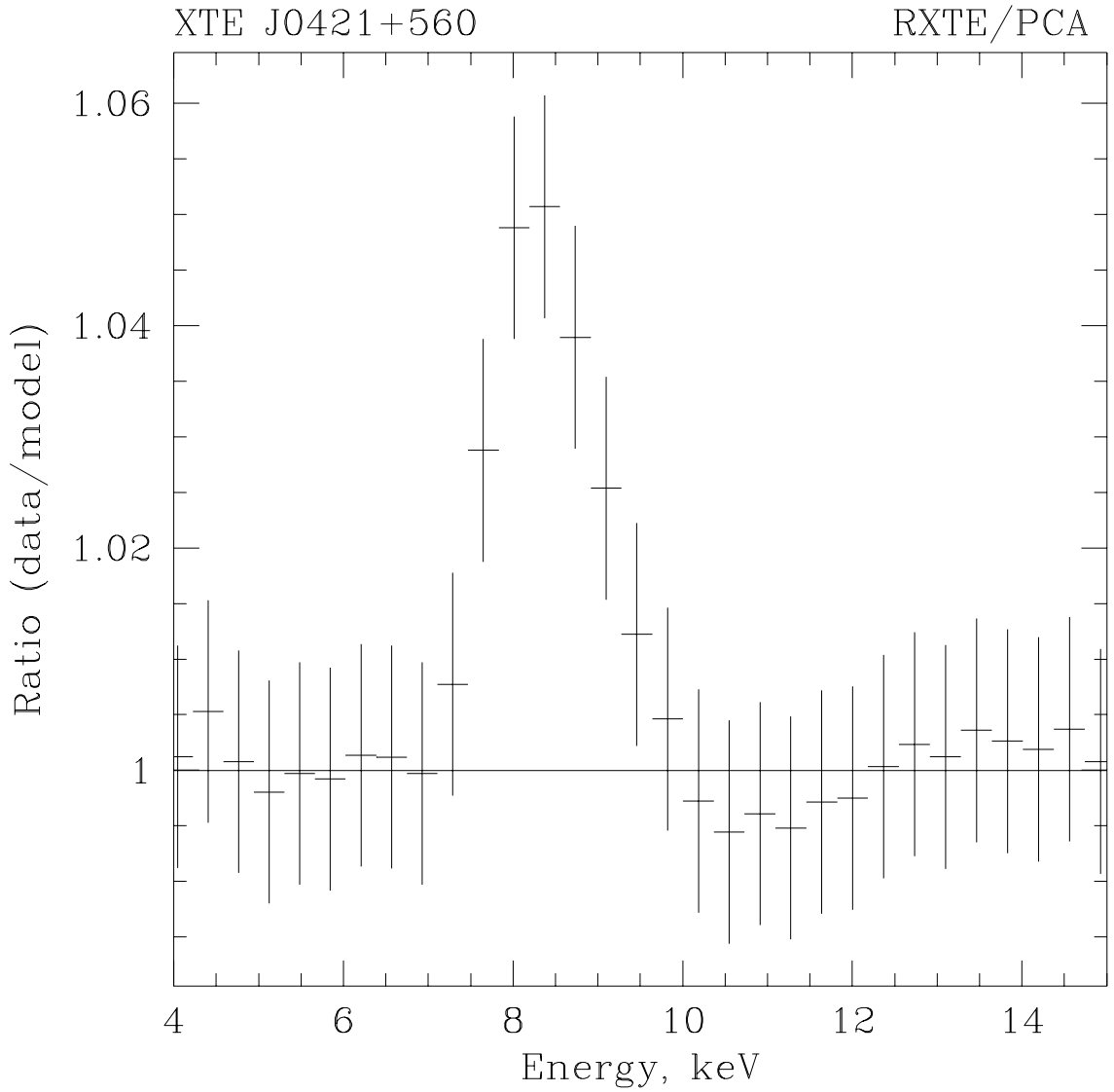

Fig. 3.— The ratio data/model, when 8 keV line was not taken into account. Systematic uncertainties of 1% are shown.

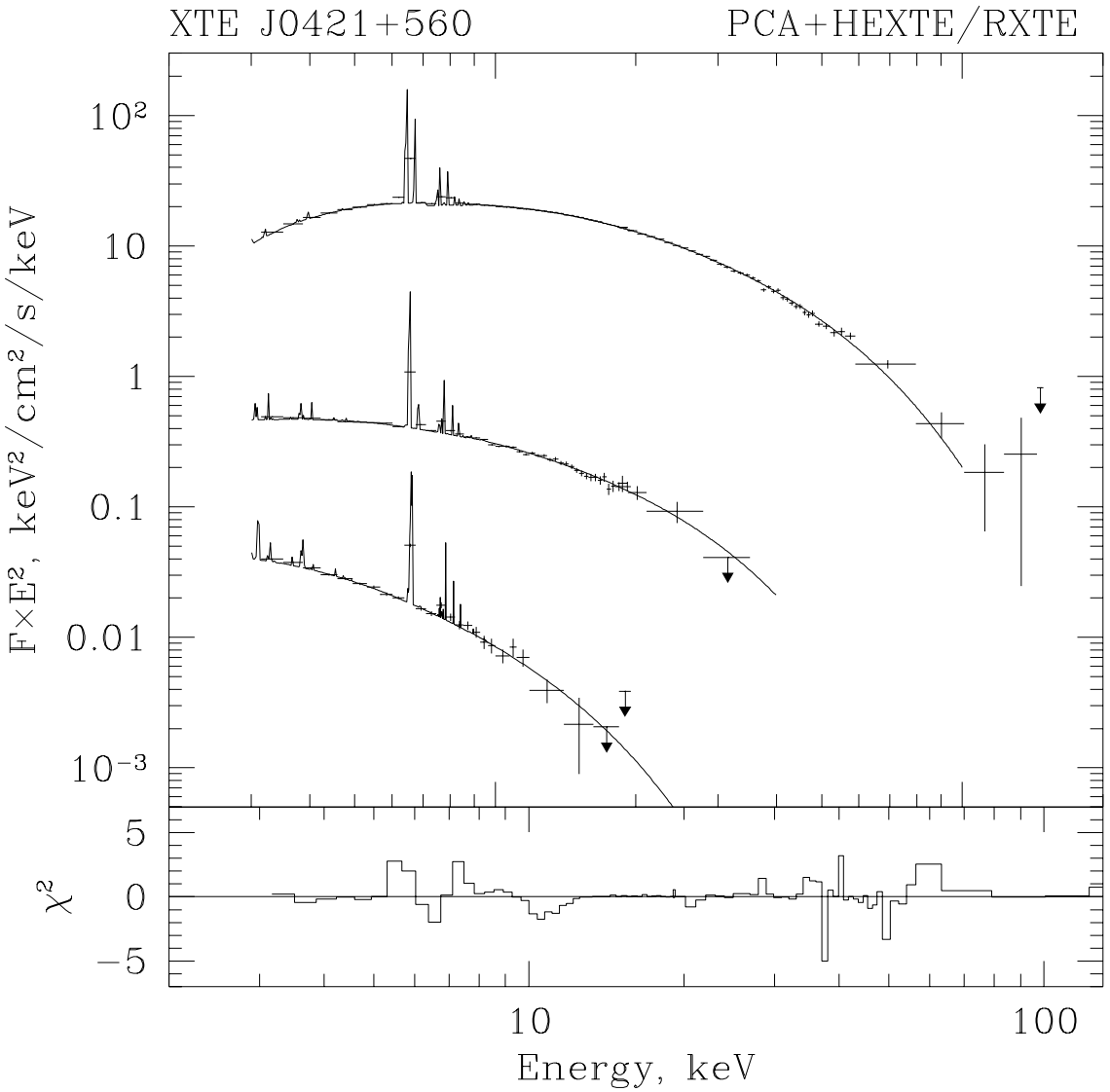

Fig. 4.— Spectra of XTE J0421+560 in different luminosity states. The most luminous one – on Apr. 1, 1998, the middle one – Apr. 3, 1998, the weakest – Apr. 9, 1998. On the lower panel the χ^2 curve for the upper spectrum is presented. Not all of shown lines are seen by PCA, a number of emission lines caused by *meka* model (see text).

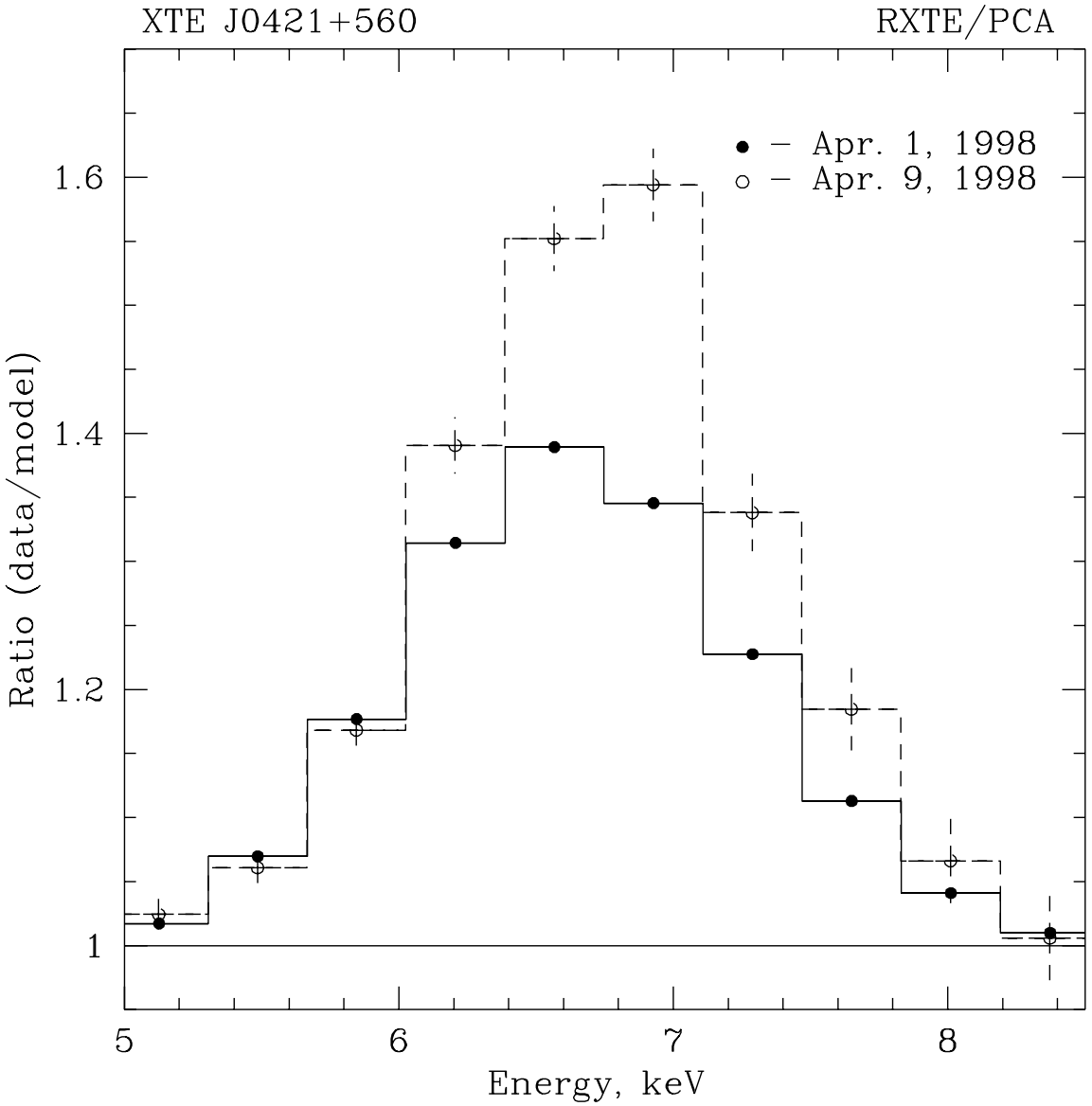

Fig. 5.— The ratio data/model when 6.5–6.7 keV line was not taken into account. One can see the shift of the line central energy.

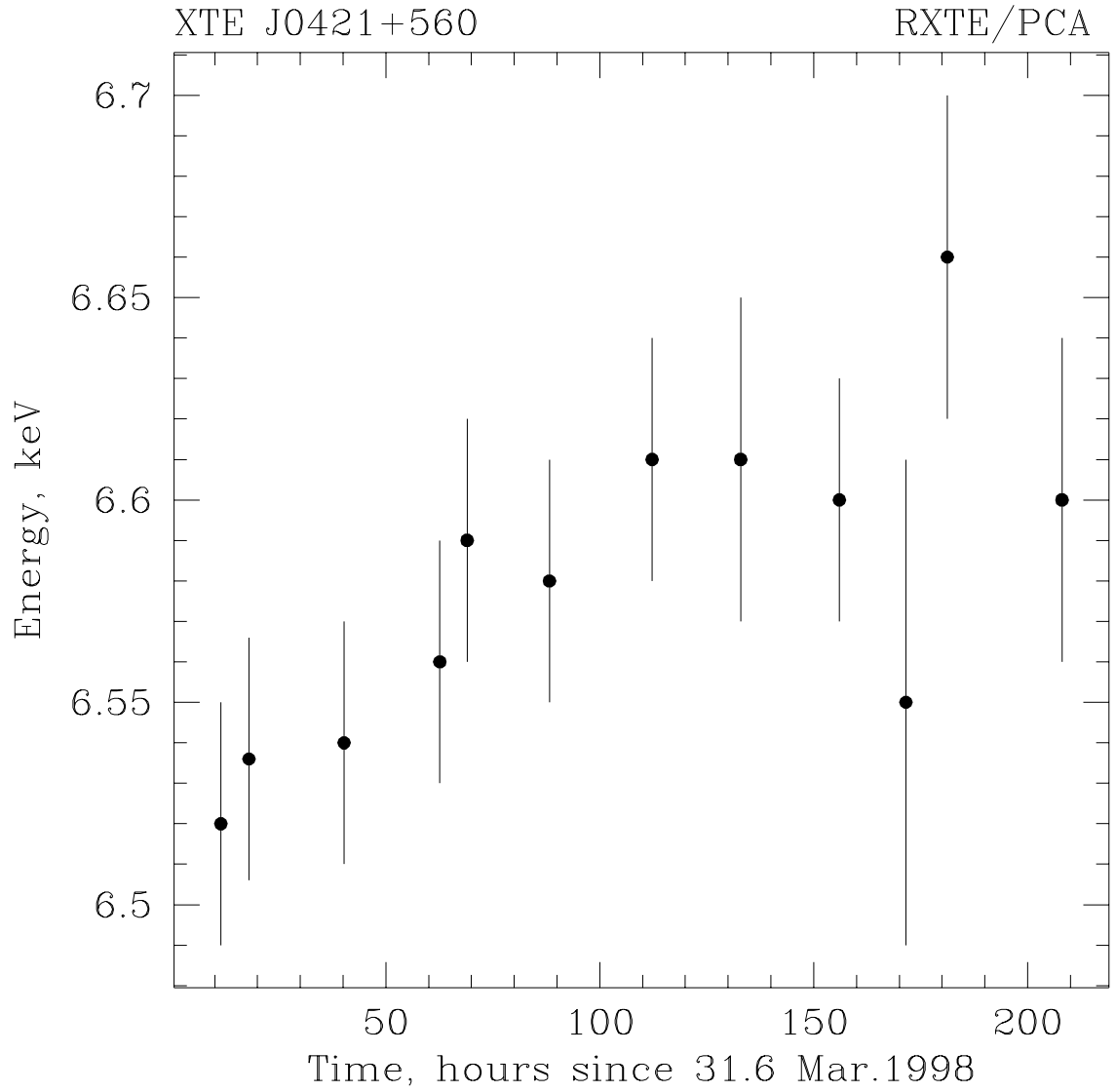

Fig. 6.— Dependence of the Fe line central energy on time.

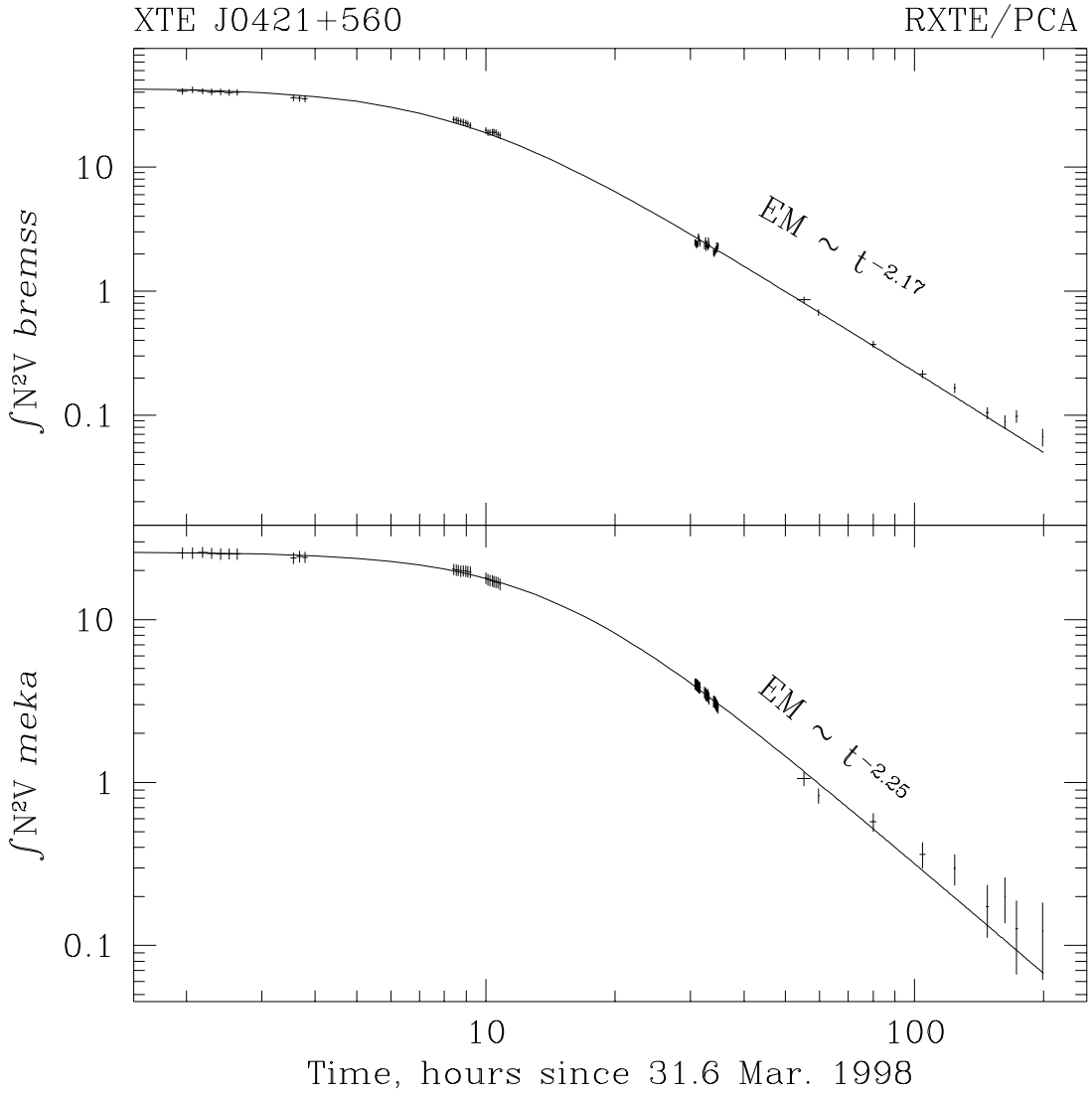

Fig. 7.— Dependence of the Emission Measures on the time for spectral two components. Solid lines show dependence $EM \sim 1/(1 + (t/\tau)^{-\alpha})$ (see text).

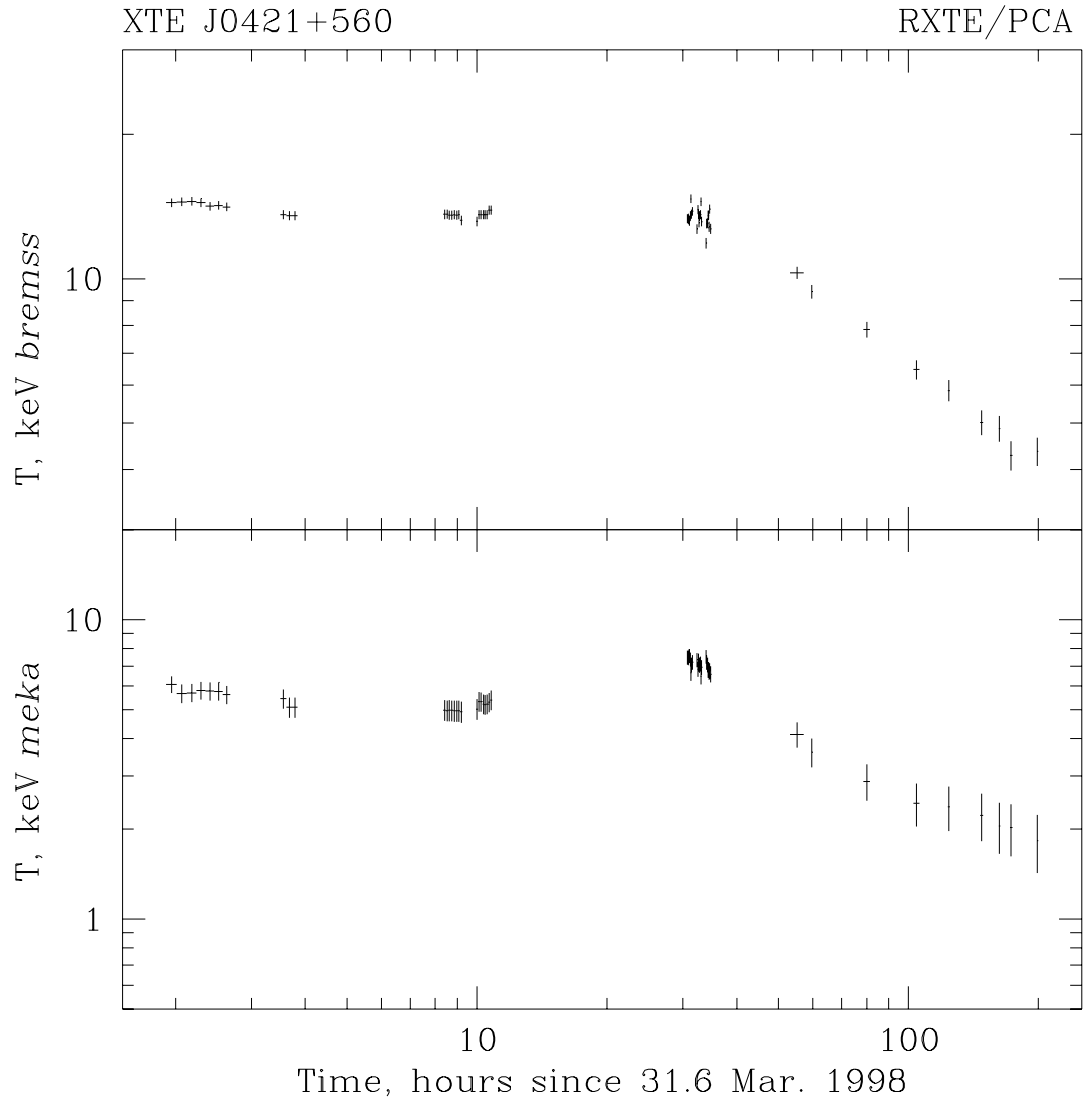

Fig. 8.— Dependence of temperatures T of two spectral components on time.

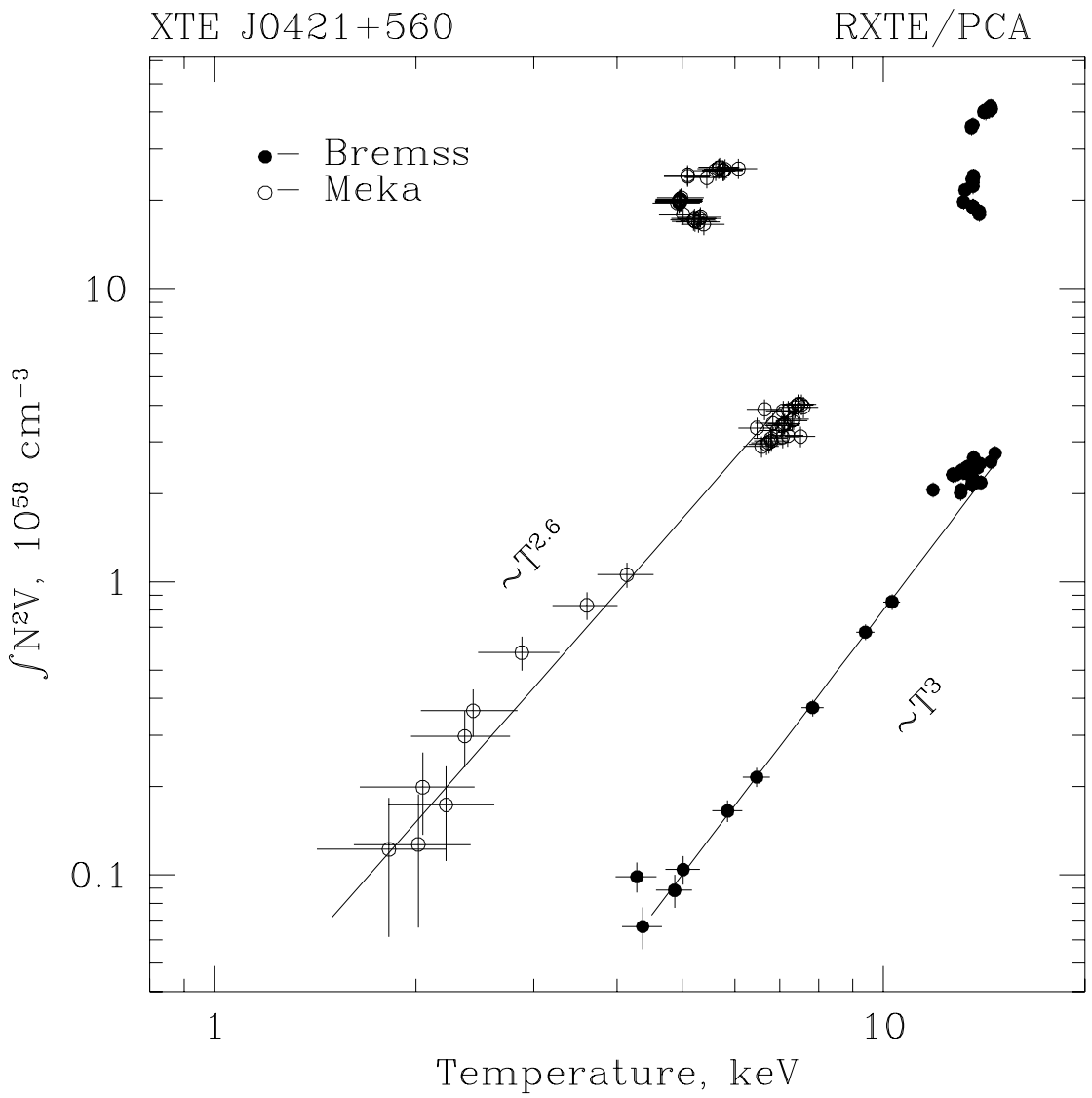

Fig. 9.— Dependence of the Emission Measures on the temperatures of two spectral components.

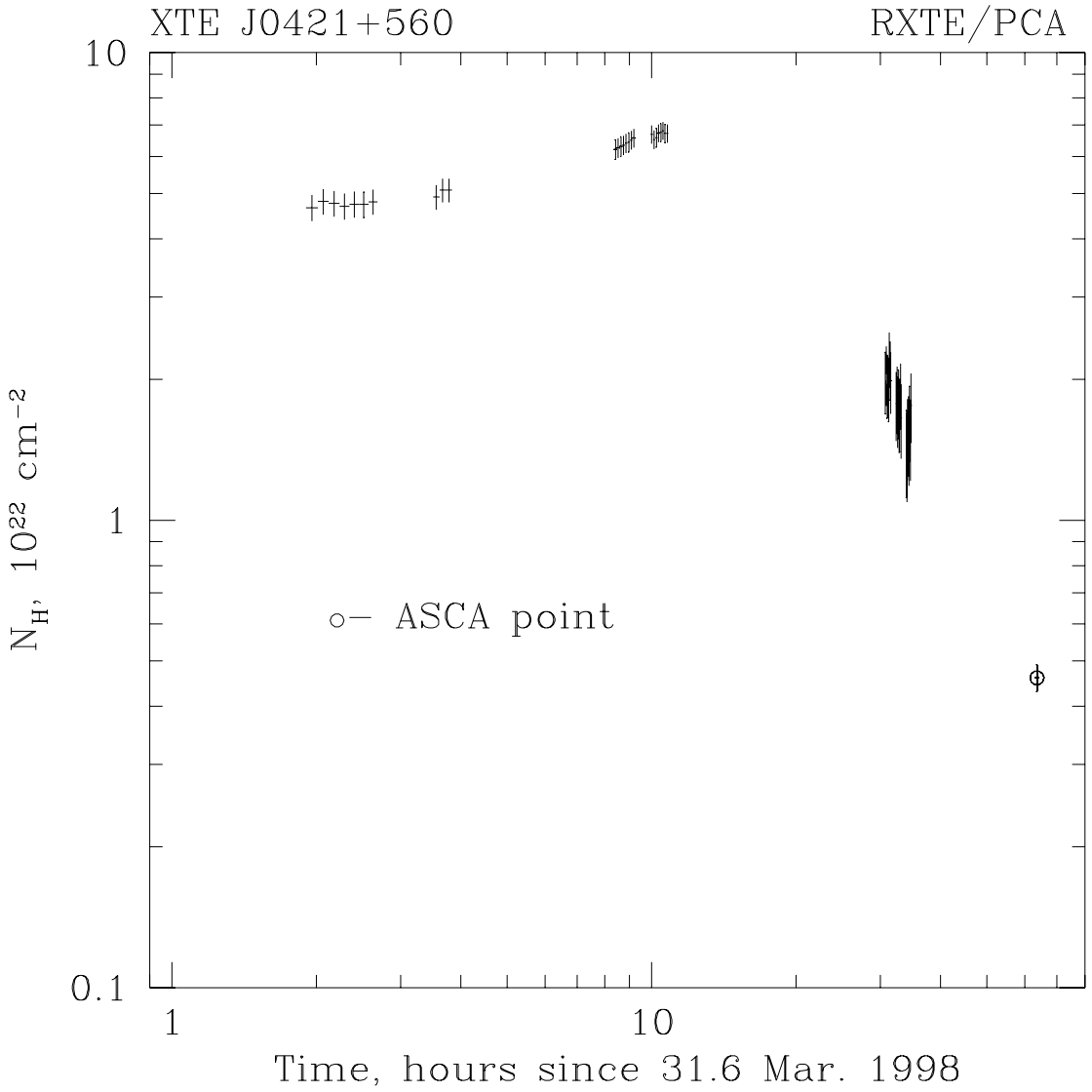

Fig. 10.— Dependence of the low energy absorption value N_H on time.

Table 1: RXTE observations of XTE J0421+560.

	Obs. ID	Date	Obs. time	Exposure, sec.	
				PCA	HEXTE[a]
1	30171-01-01-00	01/04/98	01:52:48 - 03:52:32	4109	1443
2	30171-01-02-07S	01/04/98	08:21:36 - 10:52:32	6176	4142
3	30409-01-03-00	02/04/98	06:40:32 - 10:49:36	9702	3345
4	30409-01-04-00	03/04/98	05:02:24 - 09:10:24	2740	892
5	30409-01-04-01	03/04/98	11:30:24 - 11:50:24	710	217
6	30409-01-05-00	04/04/98	06:41:20 - 09:27:28	6950	2283
7	30409-01-06-00	05/04/98	06:44:48 - 10:10:24	7590	2671
8	30409-01-07-00	06/04/98	03:21:36 - 04:30:56	1503	1016
9	30409-01-08-00	07/04/98	02:25:20 - 05:01:36	4181	1389
10	30409-01-08-01	07/04/98	18:02:08 - 18:22:56	743	191
11	30409-01-09-00	08/04/98	03:35:12 - 06:11:28	5830	2009
12	30409-01-10-00	09/04/98	06:33:20 - 07:32:32	3035	1059

[a] - Dead time corrected exposure for each claster of HEXTE detectors.

Table 2: Parameters of approximation of XTE J0421+560 spectra by a power law with high energy cutoff, two lines and absorption.

	MJD	α	E_{cut} keV	Flux (3–20 keV) 10^{-10} erg/cm^2/s	N_H 10^{22} atom/cm^2
1	50904.08	1.53 ± 0.05	12.1 ± 0.5	578 ± 11	4.8
2	50904.35	1.59 ± 0.04	11.9 ± 0.4	350 ± 7	6.5
3	50905.28	1.33 ± 0.04	9.0 ± 0.3	59.1 ± 1.2	1.5
4	50906.21	1.69 ± 0.04	9.3 ± 0.3	16.2 ± 0.3	< 1.0
5	50906.48	1.78 ± 0.05	9.2 ± 0.6	11.3 ± 0.2	< 1.0
6	50907.28	1.98 ± 0.05	8.6 ± 0.4	5.6 ± 0.1	< 1.0
7	50908.28	2.2 ± 0.1	8.0 ± 0.5	2.74 ± 0.05	< 1.0
8	50909.14	2.0 ± 0.1	6.1 ± 0.5	2.01 ± 0.08	< 1.0
9	50910.10	2.1 ± 0.4	5.4 ± 0.6	1.07 ± 0.07	< 1.0
10	50910.75	2.4 ± 0.4	$7.2^{+1.4}_{-1.6}$	0.85 ± 0.06	< 1.0
11	50911.15	2.0 ± 0.4	$4.6^{+0.7}_{-0.3}$	0.75 ± 0.06	< 1.5
12	50912.27	$2.2^{+0.3}_{-0.2}$	$5.1^{+0.9}_{-0.7}$	0.55 ± 0.06	< 1.0

– Parameter N_H is presented without errors, because of the main contribution to the uncertainty of this parameter is not the statistical one, but rather the uncertainty of respose matrix on energy range less than 4-5 keV. As usual the uncertainty of N_H value is about 1×10^{22}

Table 3: The best fit parameters of the lines (PCA data).

	Blend 6.7 keV			Blend 8 keV		
	E, keV	σ, keV	EW, eV	E, keV	σ, keV	EW, eV
1	6.52 ± 0.03	0.35 ± 0.05	559 ± 25	8.19 ± 0.14	0.1^a	77 ± 16
2	6.54 ± 0.03	0.35 ± 0.04	618 ± 23	8.20 ± 0.14	0.1^a	82 ± 14
3	6.54 ± 0.03	0.32 ± 0.04	755 ± 20	8.19 ± 0.15	0.1^a	69 ± 18
4	6.56 ± 0.03	0.28 ± 0.03	720 ± 24	8.07 ± 0.15	0.1^a	93 ± 17
5	6.59 ± 0.03	0.27 ± 0.04	736 ± 32	8.32 ± 0.15	0.1^a	102 ± 26
6	6.58 ± 0.03	0.24 ± 0.04	720 ± 38	8.04 ± 0.15	0.1^a	110 ± 27
7	6.61 ± 0.03	0.16 ± 0.04	773 ± 45	8.10^b	0.1^a	< 170
8	6.61 ± 0.04	0.23 ± 0.04	794 ± 61	8.10^b	0.1^a	163 ± 80
9	6.60 ± 0.03	0.23 ± 0.04	790 ± 60	8.10^b	0.1^a	138 ± 83
10	6.55 ± 0.06	0.35 ± 0.1	1009 ± 150	8.10^b	0.1^a	< 250
11	6.66 ± 0.04	0.21 ± 0.1	717 ± 61	8.10^b	0.1^a	174 ± 78
12	6.60 ± 0.04	< 0.25	674 ± 61	8.10^b	0.1^a	177 ± 88

[a] Parameter σ of ~ 8 keV line was fixed on the value of 0.1, because of its unresolvable width.

[b] Line position in sessions from 7 to 12 was fixed because of its weakness.

Table 4: Parameters of approximatin of PCA and HEXTE spectra by two component model, consists of model of optically thin plasma without emission lines (*bremsstrahlung*) and with emission lines (*meka*).

	kT_{bremss} keV	$\int N^2dV$ bremsshtr.	kT_{meka} keV	Red shift[a]	$\int N^2dV$ meka	χ^2 (290 dof.)
1	15.2 ± 0.2	32.3 ± 0.3	5.4 ± 0.2	0.028 ± 0.007	31.0 ± 0.4	324.68
2	13.8 ± 0.3	17.2 ± 0.9	5.1 ± 0.2	0.028 ± 0.007	17.6 ± 0.3	298.46
3	13.5 ± 0.3	2.48 ± 0.08	5.9 ± 0.2	0.029 ± 0.007	3.67 ± 0.04	280.74
4	10.1 ± 0.2	0.99 ± 0.04	4.03 ± 0.04	0.021 ± 0.007	1.37 ± 0.02	241.21
5	9.4 ± 0.3	0.65 ± 0.02	3.6 ± 0.1	0.017 ± 0.007	0.89 ± 0.03	258.72
6	7.84 ± 0.16	0.36 ± 0.01	$2.88^{+0.04}_{-0.09}$	0.012 ± 0.007	0.61 ± 0.02	269.72

– Emission measure is presented in units of 10^{58} $(\mathrm{d}/1\mathrm{kps})^2$ cm^{-3}.

– Absorbtion exists only in first, second and third sessions and equals ~ 4.8, ~ 6.6 and ~ 1.5 in 10^{22} $\mathrm{atom/cm}^2$ units respectivly.

[a] – Parameter error was fixed on 0.007 value assuming the absolute precision of energy scale 0.05 keV.